SIMS mineral/glass $^{16}O^{1}H$ calibration and tuning.

Travis Tenner[1], Marc Hirschmann[1], Richard Hervig[2]

1.University of Minnesota 2. Arizona State University

1. Background

Over the past few decades several studies have indicated that water (OH) can incorporate into the structures of nominally anhydrous upper mantle minerals (olivine, pyroxene, garnet, and their high-pressure polymorphs), as well as partial melt[1,2]. The addition of tens to hundreds of parts per million water to the bulk upper mantle assemblage can have a significant effect on its rheologic[3], seismologic[4], and petrologic[5] properties, as well as extending our views of Earth's overall water budget by several "oceans."[6] Natural specimens of the upper mantle with millimeter-sized or larger phases can have water contents easily quantified by Fourier transform infrared spectroscopy (FTIR), but often only sample the uppermost portion of the upper mantle. High P-T experimental apparati can produce hydrated upper mantle phases to much greater depth analogues, but at the expense of the phases being too small (tens of microns) to prepare and analyze by FTIR, where anisotropic minerals can only be fully quantified by taking measurements through parallel polished faces through each of the 3 optic axes. The advent of low-H background SIMS[7,8,9] has allowed for quantitative measurements of water contents in upper mantle phases as small as 50 microns in diameter, provided that OH count rates are calibrated against mineral and glass standards, each with water contents quantified by FTIR.

2. Attainment of ultra-high vacuum and low hydrogen background

* 24 hour internal bakeout
* H-free sample holder and mounting medium (indium)
* Produces a vacuum of ~ 5×10^{-10} torr.
* Produces a $^{16}O^{1}H$ background of ~10 ppm

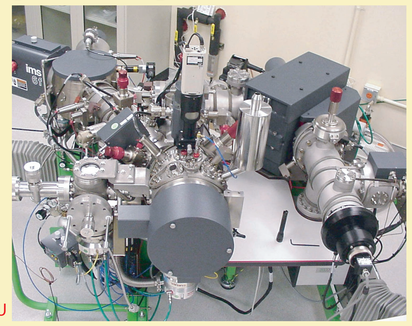

Cameca 6f SIMS at ASU

3. Standards

A total of 51 standards were used to produce phase specific calibrations on the SIMS by measuring $^{16}O^{1}H$ ions generated with a Cs^{+} primary ion beam. These standards include 7 basaltic glasses (0.35-7.65 wt% H_2O), 10 rhyolitic glasses (0.23-6.09 wt% H_2O), 14 olivines (0-910 ppm H_2O), 6 orthopyroxenes (0-263 ppm H_2O), 6 clinopyroxenes (0-490 ppm H_2O) , and 8 garnets (0-189 ppm H_2O). Water contents of the standards were quantified with unpolarized FTIR for isotropic phases (glasses and garnet), and with polarized FTIR for anisotropic phases (olivine, pyroxenes) with measurments taken along the 3 optic axes[9].

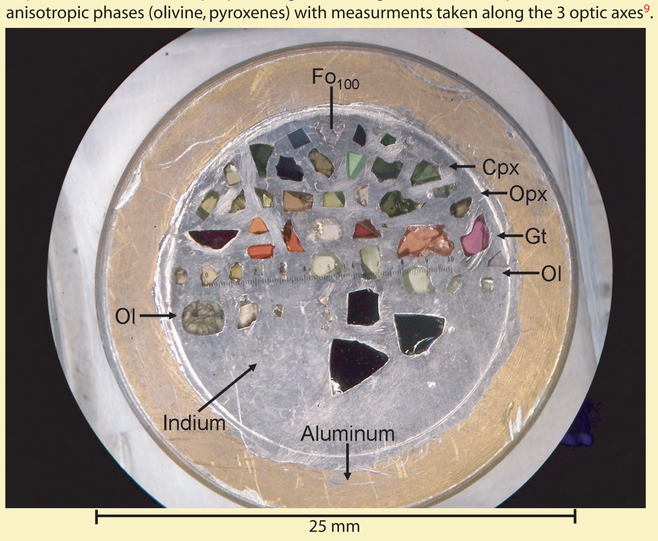

4. Primary beam alignment

Commonly, a SIMS mount will not be oriented uniformly with the ion beam, either due to slight topography across the mount, or owing to a slight tilt. This will cause the primary ion beam to "wander" from point to point across the mount even if the voltage on the steering plates of the electrostatic lens is constant. It is absolutely critical that the voltage on these plates be adjusted when the mount is moved a few hundred microns or more so that the primary beam strikes the sample in the same place (which we monitor in relation to the secondary ion optic axis) to achieve precise and accurate count rates for each measurement. We define the secondary ion optic axis as the point where the secondary ion image pinches out as the field on the secondary magnet (mass analyzer) is increased and decreased.

4a. ^{19}F Secondary ion images on indium adjacent to a standard, illustrating the secondary ion optic axis (denoted with the white reticle).

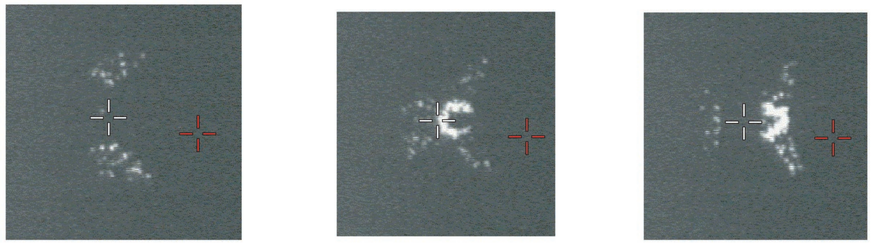

Mass analyzer adjusted to a decreased mass (vertical pinching out)

Mass analyser adjusted to the mass that produces the greatest count rate

Mass analyzer adjusted to an increased mass (horizontal pinching out)

In these images, the greatest count rate (the bright halo) is located to the right of the secondary ion optic axis, which can be "steered" back onto the secondary ion optic axis by adjusting the voltage on the primary electrostatic lens.

4b. Data collection from an aligned primary ion beam

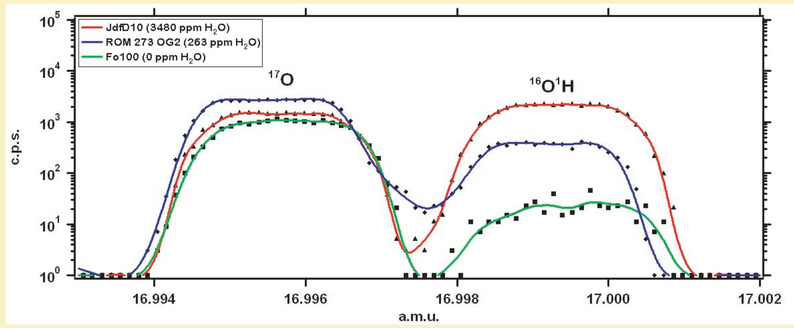

High resolution plot of log count rate versus mass for ^{17}O and $^{16}O^{1}H$ measured on basaltic glass (JdfD10), orthopyroxene (ROM 273 OG2), and the olivine standard (Fo100) which serves as a dry blank. A constant maximum count rate "plateau" is acheived with a properly aligned primary beam, yielding precise and accurate data collection.

4c. Data collection from JdfD10 with an unaligned primary ion beam

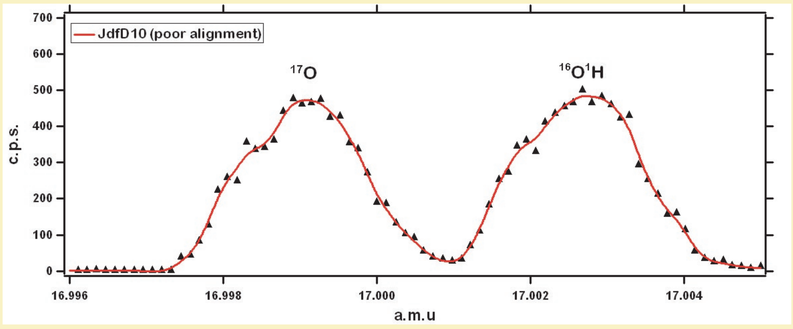

An unaligned primary beam shifts the mass where peak counts are produced, generates a reduced count rate, and does not produce a plateau across a mass range, which leads to inconsistency in mineral and glass calibration.

5. Mineral and Glass Calibration

We plot the FTIR-determined water content of the standards against the $^{16}O^{1}H/^{30}Si$ count rate ratio multiplied by the SiO_2 content determined from electron microprobe analyses of the standards. The mass analyzer was tuned using ^{18}O to minimize the Bxa effect on the count rates of $^{16}O^{1}H$ and ^{30}Si.

This form of plotting allows us to both visualize the water contents of each standard, while also comparing standards of a different normalizing element (SiO_2), which allows us to investigate any matrix effects during SIMS analyses of $^{16}O^{1}H$.

5a. Glass Calibration Curves

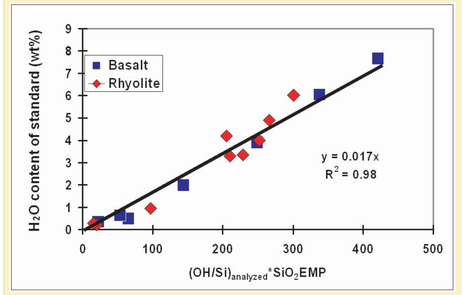

5b. Mineral Calibration Curves

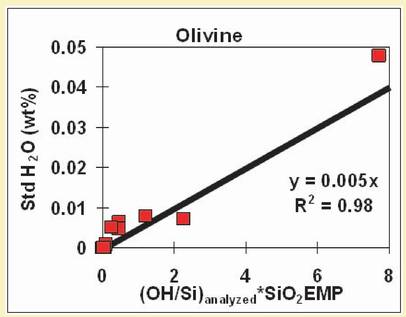

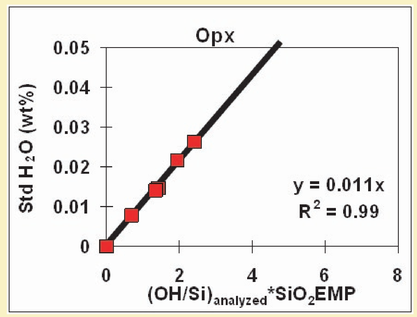

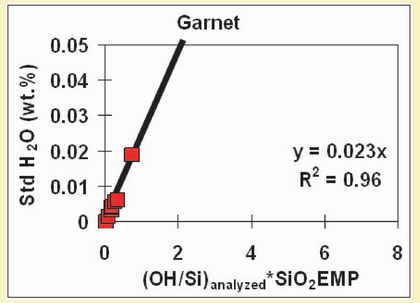

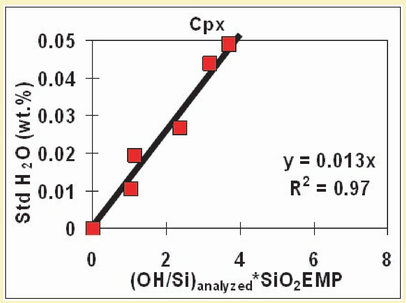

5c. Matrix effects during SIMS analysis of $^{16}O^{1}H$

As evidenced by the linear, well-resolved curves of equal slope for rhyolitic and basaltic glasses, as well as near-identical slopes of the curves for clinopyroxene and orthopyroxene crystals, we find no intraphase matrix effect on the SIMS calibration of $^{16}O^{1}H$. However, there is a significant interphase matrix effect, as olivine, pyroxene, garnet, and glass each produce a calibration curve with a unique slope.

6. References

1. Beran A. and Putnis A. (1983) Phys Chem Minerals, 9, 57-60.
2. Bell D. R. and Rossman G. R. (1992) Science, 255, 1391-1397.
3. Hirth G. and Kohlstedt D. L. (1996) Earth Planet Sci Lett, 144, 93-108.
4. Karato S-I. and Jung H. (1998) Earth Planet Sci Lett, 157, 193-207.
5. Gaetani G. A. and Grove T. L. (1998) Contrib Mineral Petrol, 131, 323-346.
6. Hirschmann M. M. (2006) Annu Rev Earth Planet Sci, 34, 629-653 .
7. Koga K. et al. (2003) Geochem Geophys Geosys, doi: 10.1029/2002GC000378.
8. Hauri E. H. et al. (2006) Earth Planet Sci Lett, 248, 715-734.
9. Aubaud C. et al. (2007) Am Mineral, 92, 811-828.